A Study of the Flow Phenomenon of Water in a Channel with Flat Plate Obstruction Geometry at the Entry

M. A. Kabir, M. M. K. Khan*
James Goldston Faculty of Engineering and Physical Systems, Central Queensland University, North Rockhampton, QLD-4702, Australia
M. A. Bhuiyan
Faculty of Civil Engineering, Bangladesh University of Engineering and Technology, Dhaka-1000, Bangladesh

The flow in a parallel walled test channel, when obstructed with a geometry at the entrance, can be forward, reverse and stagnant depending on the position of the obstruction. This interesting flow phenomenon has potential benefit in the control of energy and various flows in the process industry. In this experiment, the flat plate obstruction geometry was used as an obstruction at the entry of the test channel. The parameters that influence the flow inside and around the test channel were the gap (g) between the test channel and the obstruction geometry, the length (L) of the test channel and the Reynolds number (Re). The effect of the gap to channel width ratio (g/w) on the magnitude of the velocity ratio (V_I/V_O: velocity inside/ velocity outside the test channel) was investigated for a range of Reynolds numbers. The maximum reverse flow observed was nearly 20% to 60% of the outside velocity for Reynolds number ranging from 1000 to 9000 at g/w ratio of 1.5. The maximum forward velocity inside the test channel was found 80% of the outside velocity at higher g/w ratio of 8. The effect of the test channel length on the velocity ratio was investigated for different g/w ratios and a fixed Reynolds number of 4000. The influence of the Reynolds number on the velocity ratio is also discussed and presented for different gap to width ratio (g/w). The flow visualisation photographs showing fluid motion inside and around the test channel are also presented and discussed.

Key Words: Reynolds Number, Reverse Flow, Velocity Ratio, Gap to Width Ratio, Test Channel and Flat Plate Obstruction

1. Introduction

The flow pattern of water in a channel, referred to as test channel, with an obstruction at the entry placed in another wider channel was studied by Bhuiyan et al. (2000) and Kabir et al. (2002). The flow inside the test channel can be forward, reverse or stagnant depending on the several flow parameters. The investigation of the flow of water inside and around the test channel with obstruction at the entrance has attracted much attention due to their industrial applications. Earlier study (Kabir et al 2002) on various obstruction geometries namely circle, triangle, rectangle (flat plate of different thickness) and semicircle for water observed that flat plate (8 mm thick) obstruction produces the maximum reverse flow than other shapes of obstruction geometry. Therefore, the flat plate (8 mm thick) obstruction geometry was chosen to study the influence of different flow parameters. The parameters that were known to

* Corresponding Author,
E-mail : m.khan@cgu.edu.au
TEL : +61-7-4930-9381; **FAX** : +61-7-4930-9382
James Goldston Faculty of Engineering and Physical Systems, Central Queensland University, North Rockhampton, QLD-4702, Australia. (Manuscript **Received** July 18, 2002; **Revised** March 26, 2003)

affect the flow inside and around the test channel are the gap (g) between the test channel and the obstruction geometry, the length (L) of the test channel and the Reynolds number (Re).

This flow phenomenon has potential benefit and can be employed in the control of energy and various flows in process industry. Some of the applications where this type of flow phenomenon can occur or can be employed are in the control of flow to obtain low velocities; heat transfer problems providing different types of flows locally; interaction of shear layers at varying distance apart; flow past obstructions and constrictions in arterial flows under certain physiological situations.

Bhuiyan et al.(2000) and Kabir et al.(2002) studied this interesting flow phenomenon and attempt has been made by the authors to investigate this flow phenomenon in more details using flat plate obstruction geometry. There are investigations where Gowda et at (1993) studied flow phenomenon of fluids in a channel with obstruction at relatively low Reynolds number. There exist some other investigations, which dealt with control of flow using different types of valves (Streeter 1961; Davis and Sorenson 1969; Eom 1988). There are investigations dealing with the mechanism of vortex formation and shedding (Gerrard 1966, 1978) and the interaction of two shear layers with different spacing in between (Abernathy and Kronauer, 1962). Bearman and Truman (1972) investigated the flow around cylinders of different length to width ratio. You et al.(2000) studied the constant mass flow rate in fully developed channel and pipes. Val Healy (1992) studied the control of turbulent flow on a backward facing step. Unal and Rockwell (1988a, b) investigated the vortex shedding process and the influence of a splitter plate behind a circular cylinder. Park et al.(2002) studied the two dimensional flow with moving free surface.

Earlier work by Kabir et al (2002) mainly concentrated on different size and shapes of obstruction geometry. They studied the influence of the size and shapes of the obstruction geometry on the flow feature for a fixed Reynolds number.

To study the flow features inside and around the test channel in more details, different flow parameters were investigated. They were the gap (g) between the obstruction geometry and the test channel, the length (L) of the test channel and the Reynolds number (Re) based on the channel width (w) and the outside velocity (V_o). For simplicity of the experiment, the depth of the fluid (water) in the channel was kept constant at 130 mm. These parameters varied and their influences on the velocity ratios (V_i/V_o: velocity inside/outside the test channel) were studied.

2. Materials and Equipment

The materials and equipment used in this experiment were water, open channel rig with different test channel length, flat plate obstruction geometry, pitot-static tube connected with a pressure transducer and the Lab-View program, timica and aluminium particles, halogen lights, high-speed digital camera, thermometer and a variable-speed motor pump.

3. Experimental Procedure

A tank of 3.0 m long×0.9 m wide×0.25 m deep was designed and fabricated with 3 mm galvanised steel sheet. An open channel rig was made by placing the two guides of 2.0 m long×0.2 m wide×0.25 m deep at the middle of the tank with a gap of 300 mm in between them, where the test channel was placed with a flat plate obstruction at the entrance. A small reservoir of 0.4 m long× 0.2 m wide×0.6 m deep attached at one end of the tank was connected with the suction side of the pump. This small reservoir holds enough volume of water to be drawn by the suction end of the pump during operation. The delivery end of the pump was split into two parts and was connected at the reservoir tank side. The pump was driven by a variable speed d.c. motor that produced a range of velocities in the test section of the channel. The suction end collected the water that flowed through a single channel (test section) into the small reservoir while the delivery end of the pump delivered water through the two split parts into the tank. The flows from the delivery end of the

pump were guided into the opposite side of the tank where two flows intermingled together and then continue as a single flow through the test section. The schematic diagram and photograph of experimental rig are shown in Figures 1 and 2 respectively.

A pitot-static tube, calibrated against video camera velocity measurement technique, (Bhuiyan et al., 2000) was used to measure the fluid velocity inside and outside the test channel. The velocity obtained by the video camera measurement technique was the surface velocity measured by tracking the distance travelled by the plastic beads along the central region of the test channel. The pitot-static tube, placed 5 mm beneath the water surface, was connected to a pressure transducer of 0-2 mbar to measure the velocity. A 'Lab-view' program, linked to a pressure transducer, recorded and displayed the water velocity measured by the pitot-static tube through an appropriately written program. The pitot static tube results were found to 3-5% higher than the velocities measured by the video camera and were considered acceptable. This lower magnitude measured by video camera technique may be attributed to the friction between the plastic beads and the air.

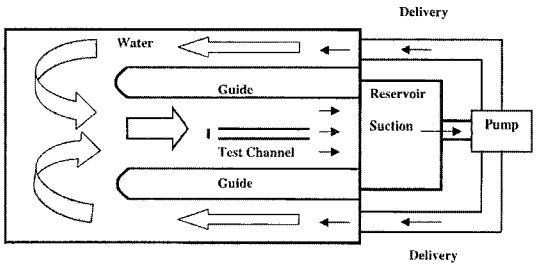

Fig. 1 Schematic diagram of experimental set up

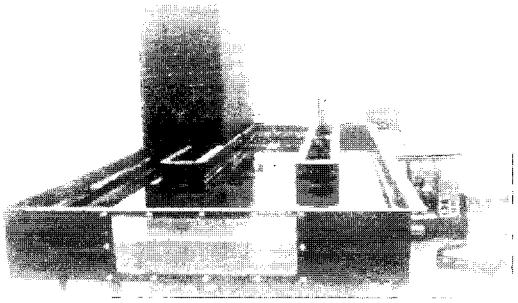

Fig. 2 Photograph of experimental set up

In all cases inside (V_I) and outside (V_O) velocities of the test channel were measured several times (average 10 times) and the mean values were taken. To avoid any variation of the water properties, the experiment was conducted at a constant temperature of 25℃.

Fluid used in this experiment was water. It was observed that the depth of water in the channel remained fairly constant during the experimentation. The fine timica and aluminium particles were mixed with water and used as tracer medium. These tracer particles were chemically inert. The two halogen lights were placed inside the guides to illuminate the particles flowing through the channel showing the flow pattern. A Nikon broadways high-speed digital camera was used to take flow visualization photographs. The camera was positioned at a suitable location above the test section of the open channel rig. The exposure time of the photographs was 1/8 of a second. The aperture for 1/8 second of exposure time was f/5.6 at 60 mm focal length. The most important flow features appeared to occur in the regions near the entry and exit of the test channel. Only the entry and exit photographs were taken to capture the flow field details of a manageable length and are presented here.

The schematic diagram of the test channel is shown in Figure 3. The width of the test channel (w) and the breadth of the obstruction (b) were constant and equal to 25 mm. The thickness (l) to breadth (b) ratio (l/b) of the flat plate obstruction geometry was equal to 0.32. The flat plate geometry with l/b ratio of 0.32 was seen to produce the maximum reverse flow (Kabir et al.,

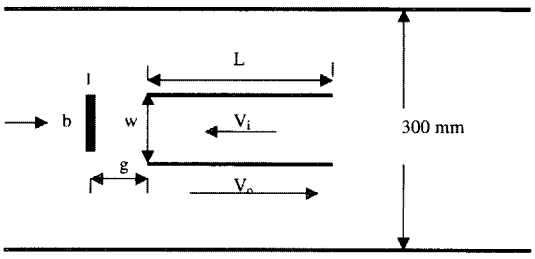

Fig. 3 Test channel

2002) for water. Thus the flat plate was chosen for investigation into the influence of different flow parameters on the velocity ratios.

The gap width (g) was varied from 12.5 mm to 200 mm, giving a range of g/w ratios from 0.5 to 8. The investigation was carried out for four sets of test channel lengths (L) namely, 200 mm, 300 mm, 400 mm and 500 mm. Results of only two set channel lengths (300 mm and 500 mm) are presented for brevity. For each set of test channel length, investigation was carried out for Reynolds number of 1000, 2000, 3000, 4000, 6000 and 9000.

The effect of the test channel length (L) on the flow phenomenon was studied for g/w ratio ranging from 0.5 to 8.0 and a constant Reynolds number of 4000. The influence of Reynolds number (Re) on the velocity ratio (V_i/V_o) was also investigated for different set of test channel lengths (L) (L=200 mm, 300 mm, 400 mm and 500 mm giving L/w=8, 12, 16 and 20) but results of only two-test channel lengths (300 mm and 500 mm) are presented here for brevity. For every set of test channel length, investigation was carried out for varying g/w ratios ranging from 0.5 to 8.0.

4. Results and Discussions

The flow parameters have significant influence in determining the flow behaviour of water inside and around the test channel. Influence of those parameters are presented and discussed here systematically. Results of those parameters are presented here against the velocity ratio (V_i/V_o: velocity inside/velocity outside the test channel).

In this experiment, Reynolds number was calculated using the formula

$$Re=\rho w V_o/\mu \qquad (1)$$

Where V_o is the surface velocity outside the test channel, w is the width of the test channel, ρ is the density of water and μ is the viscosity of water.

4.1 Influence of gap g

The investigation was carried out for different test channel lengths (L) of 200 mm, 300 mm, 400 mm and 500 mm. Each test length was tested at g/w ratio of 0.5, 1, 1.5, 2, 3, 4, 5, 6, 7 and 8 for Reynolds numbers ranging from 1000 to 9000. The influence of the gap to width (g/w) ratio on the velocity ratio (V_i/V_o) is shown in Figures 4 (a) and (b) for test channel lengths of 300 mm and 500 mm respectively. A negative (−) value of the velocity ratio indicates a reverse flow whereas a positive (+) value indicates a forward flow. The important flow features that occurred in the test channel were at the entrance and exit ends. The flow visualisation photographs of both ends were taken to capture and investigate the flow features. Since the central part of the test channel is not included in the photographs, the entry and exit photographs are pasted side by side leaving a small gap between them (Figure 5(a) ~ (e)). These flow visualization photographs show the flow pattern at Reynolds number 6000 for L/w ratio 12.0 (L=300 mm). It is noted that the flow visualisation pictures shown in Figure 5 (a) ~ (e), have the same flat obstruction geometry but its aspect ratio appears different due to length and width magnification and adjustment in the picture frame for clarity of the flow features. The

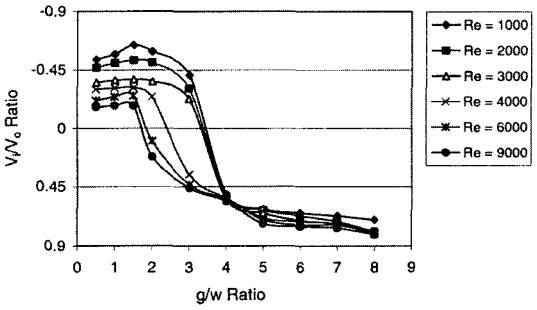

Fig. 4(a) g/w vs. V_i/V_o for L/w=12

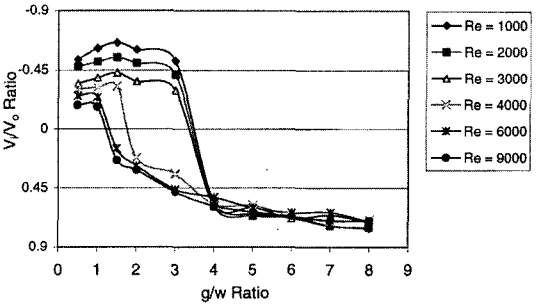

Fig. 4(b) g/w vs. V_i/V_o for L/w=20

appropriate length and width ratio (XY coordinates) for each picture is shown in the respective photograph (Figure 5(a) ~ (e)).

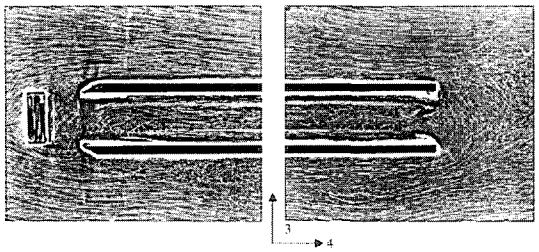

(a) g/w=0.5, Re=6000 and L/w=12.0

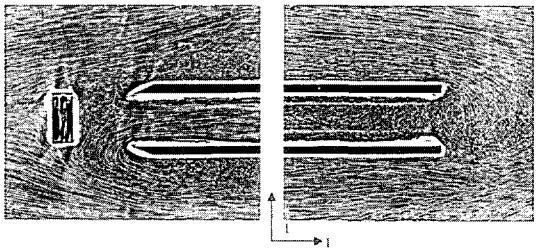

(b) g/w=1.0, Re=6000 and L/w=12.0

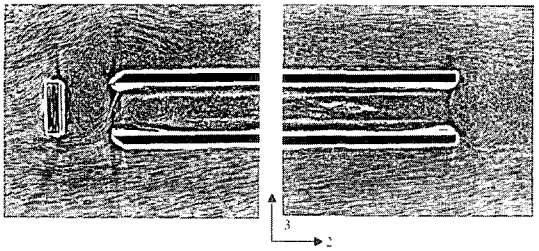

(c) g/w=1.5, Re=6000 and L/w=12.0

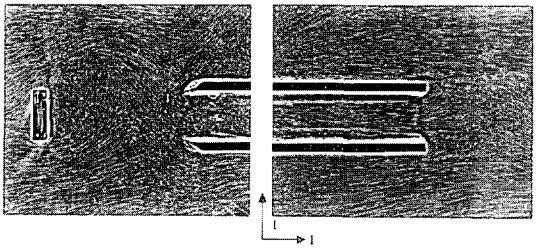

(d) g/w=3.5, Re=6000 and L/w=12.0

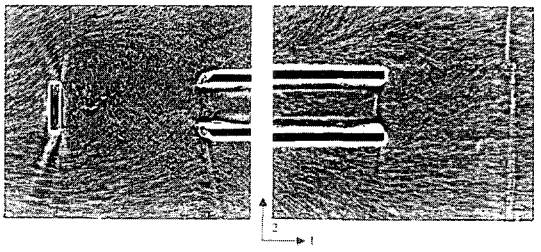

(e) g/w=6.0, Re=6000 and L/w=12.0

Fig. 5 Flow pattern at different g/w ratios

At low g/w ratio (g/w=0.5), the flow inside the test channel is reverse to that of the outside flow. As the g/w value increases the magnitude of the reverse flow increases until it reaches a maximum at g/w ratio of 1.5. Typical flow visualisation photographs were taken at g/w ratios of 0.5, 1.0 and 1.5 showing reverse flow phenomenon (Figures 5(a), (b) and (c)). With further increase in g/w ratio, the reverse flow weakens and the flow in the test channel is observed stagnant or a slow forward motion at g/w ratio of 2.0 to 3.5. A typical flow visualisation photograph taken at g/w ratio of 3.5 showing flow features inside and outside the test channel is presented in Figure 5(d). Again as g/w ratio increases a forward motion is observed, which strengthens as g/w ratio increases.

When obstruction geometry is placed ahead of the test channel a region of low pressure developed behind the obstruction and this low pressure triggers the flow in reverse direction inside the channel. The shear layers at the front and rear ends on both sides of the channel become unstable and roll up giving rise to complex vortex shedding. This vortex regulates the flow of the water through the channel. The magnitude of the reverse flow is determined by the combination of the low pressure behind the obstruction and the strength of the vortex shedding (Kabir et al., 2002). Although there was a vortex shedding at the entrance and exit of the test channel overall flow in the wider channel observed was steady. This was confirmed by injecting dye, and a careful measurement and monitoring of the flow in the wider channel.

In flow visualization photographs Figure 5(a), (b) and (c), it can be seen that at small gap (g/w ratio ranging from 0.5 to 1.5), shear layers from the edges of the flat plate bound to reattach the sidewalls of the test channel. These give rise to low pressure at the gap triggering the flow in the reverse direction through the test channel. As gap increases, the shear layers can now roll up into the gap, which reduces the magnitude of the negative pressure behind the flat plate obstruction. This causes the reverse flow to weaken and

stop or flow forward. A typical photograph of a slow forward flow can be seen in Figure 5(d) taken at g/w ratio of 3.5. With further increase in gap, stronger forward flow inside the test channel was observed and flow visualization picture taken at g/w ratio of 6 is presented in Figure 5(e) showing a forward flow.

The maximum reverse flow in the channel is observed at low g/w ratios and the magnitude of the velocity ratio is around 20% to 60% of the outside velocity for a range of Reynolds numbers from 1000 to 9000. At low g/w ratio, the magnitude of the reverse flow is higher for lower Reynolds number. At high g/w ratio for example 8, the flow inside the channel is observed forward. The magnitude of the forward flow inside the test channel is approximately 65% to 80% of the outside velocity for a range of Reynolds numbers. The flow visualization photographs of 300 mm channel length only are presented, as these for other channel lengths (300 mm, 400 mm and 500 mm) appeared almost similar.

4.2 Influence of length L

The Influence of the test channel length on the velocity ratio (V_I/V_o) was investigated for a set of g/w ratios (from 0.5 to 8.0) and for a fixed Reynolds number of 4000. The test channel lengths (L) used in the experiment were 200 mm, 300 mm, 400 mm and 500 mm (L/w=8, 12, 16 and 20). Figure 6 presents the influence of L on the magnitude of the velocity ratio (V_I/V_o). The flow visualization photographs were taken at channel lengths (L) of 200 mm and 500 mm (L/w ratio=8 and 20) for g/w ratio of 1.5 and are presented in Figure 7. It is seen from Figure 6 that the reverse flow occurs for low g/w ratios (0.5, 1 and 1.5) and decreases slightly with increase in L/w ratio. An interesting flow feature is noticed for g/w ratio of 2. In particular, the reverse flow which is observed for lower L/w ratio, suddenly begins to weaken at L/w ratio of 12 until the flow becomes stagnant at L/w ratio of 14, with further increase in L/w ratio, the flow becomes forward. Forward flow is observed for higher g/w ratios (3 to 8) at L/w ratio ranging from 8 to 20. Forward flow slightly increases initially with increasing L/w ratio and reaches almost constant with further increase in L/w ratio.

This shows that for lower and higher g/w ratio (except for g/w=2) the flow trend is almost unaffected by L/w ratios. It is seen in flow visualization photographs that for all set of channel length L/w ratio ranging from 8 to 20 the shear layers separating from the front plate extend almost to the end of the test channel and a strong recirculating flow is observed. The reverse flow inside the channel is caused by the low base pressure behind the obstruction geometry at the entry and it is expected that the velocity in the reverse direction would decrease slightly as the length of the test channel increases. The vortices were observed at the both ends for all L/w set of geometries. The strength of the vortices and pressure behind the flat plate are unknown. The flow pattern at the two ends appeared to have changed with the change of test channel length as

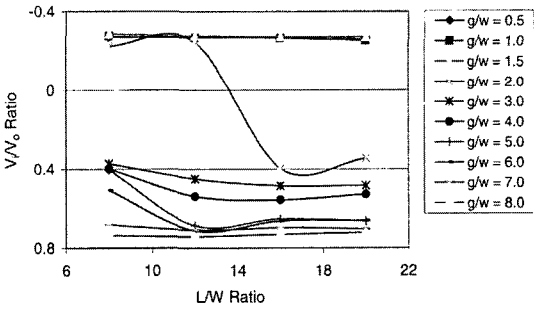

Fig. 6 V_I/V_o Vs L/w for Re=4000

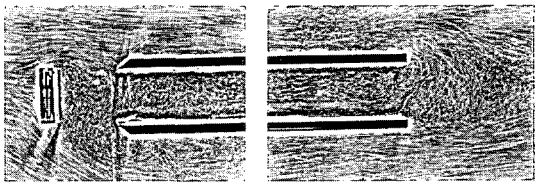

(a) L/w=8 (L=200 mm), Re=4000, g/w=1.5

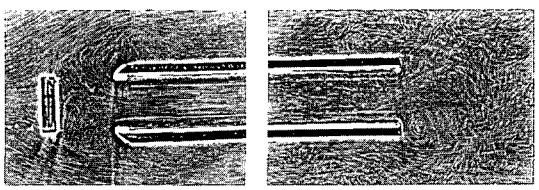

(b) L/w=20 (L=500 mm), Re=4000, g/w=1.5

Fig. 7 Flow pattern of two different test Channels

shown in flow visualization photographs (Figure 7(a) and (b)).

4.3 Influence of reynolds number Re

The influence of the Reynolds number on the magnitude of the velocity ratio (V_i/V_o) is investigated for different set of test channel lengths (L) of 200 mm, 300 mm, 400 mm and 500 mm. For each test channel length, the gap (g) was varied from 12.5 mm to 200 mm giving a g/w ratio of 0.5 to 8.0. For brevity, the results of the two test channel lengths of 300 mm and 500 mm (L/w= 12 and 20) are presented and discussed. Figures 8 (a) and (b) present the influence of Reynolds number on the velocity ratio (V_i/V_o).

For lower g/w ratios, a strong reverse flow occurs at low Reynolds number for both L/w ratios of 12 and 20 and as Reynolds number increases the reverse flow weakens and continues to decrease with further increase in Reynolds number. For higher g/w ratios, the flow is forward for both L/w ratios and its value increases slightly with increase in Reynolds number and becomes almost constant with further increase.

An interesting flow feature is noticed for g/w ratios of 2 and 3 for L/w ratio of 12. The reverse flow, which is observed at low Reynolds number, starts to weaken at 3000 and 4000 respectively, until it reaches to a stagnant flow at Reynolds numbers of 3500 and 5500 respectively. With further increase in Reynolds number the flow turns to forward. Likewise the reverse flow turns to stagnant for g/w ratio 1.5, 2.0 and 3.0 at Reynolds number 3500, 3600 and 5500 for higher L/w ratio of 20.

The flow visualization photographs taken at Reynolds number of 1000, 2000, 3000, 6000 and

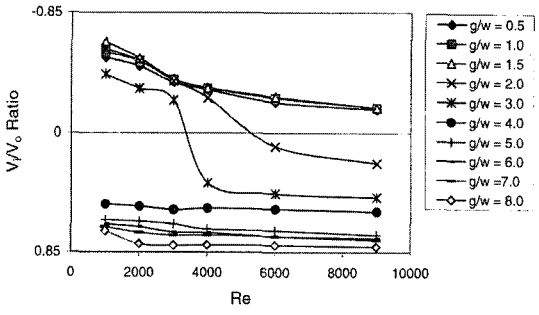

Fig. 8(a) Re vs. V_i/V_o for L/w=12

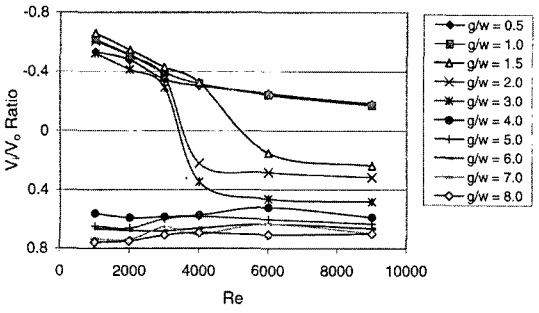

Fig. 8(b) Re vs. V_i/V_o for L/w=20

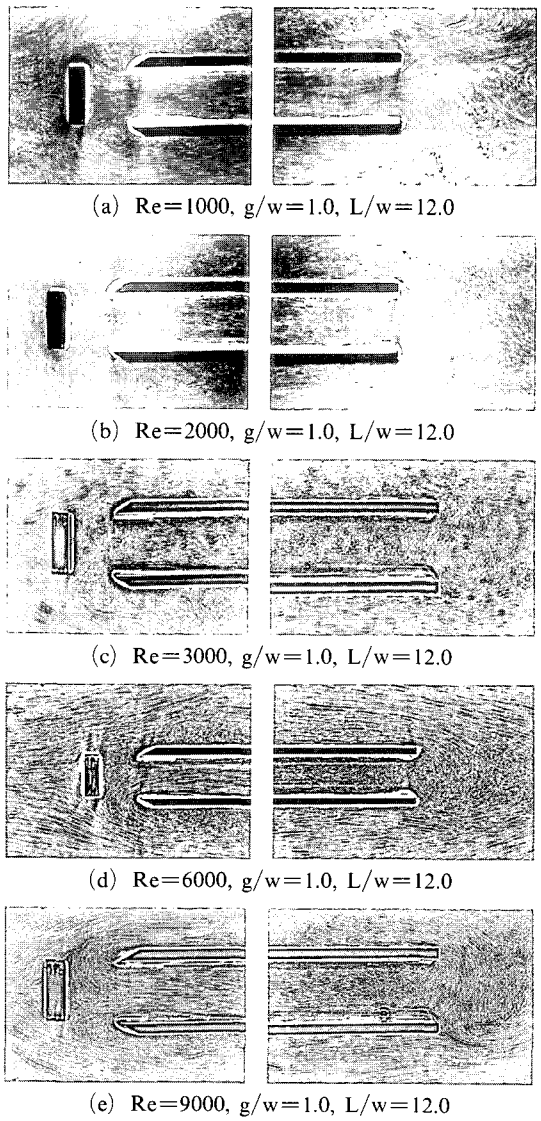

(a) Re=1000, g/w=1.0, L/w=12.0

(b) Re=2000, g/w=1.0, L/w=12.0

(c) Re=3000, g/w=1.0, L/w=12.0

(d) Re=6000, g/w=1.0, L/w=12.0

(e) Re=9000, g/w=1.0, L/w=12.0

Fig. 9 Flow pattern at different reynolds number

9000 are presented in Figure 9(a) ~ (e) for L/w ratio of 12.0 and g/w ratio of 1. 0. The vortices are clearly visible at both entry and exit ends and with increasing Reynolds number vortex pattern changes at both ends. It is known (Bearman and Trueman, 1972) that two free shear layers, free to interact, are basically unstable and roll up to form discrete vortices. During the formation of the growing vortices and, to a much lesser extent, the shear layers draw in water from the base region and it is suggested that it is this continual entrainment process that sustains the low base pressure. The removal of entrained water is balanced by an induced reverse flow into the formation region. The base pressure determines the amount of vorticity that is being shed from each side of the body and this in turn is related in some way to the distance to vortex formation and the strength of the fully formed vortices (Bearman and Trueman, 1972).

From this investigation it was seen that the reverse flow phenomenon occurs at Reynolds number ranging from 1000 to 9000. In other words, the reverse flow phenomenon was observed to occur in both laminar and turbulent flow. These results somewhat contradict that of Gowda et al. (1989). Gowda et al.(1989) reported the existence of the reverse flow phenomenon for turbulent flow of Reynolds number greater than 2000.

Results found in this experiment are nearly similar to that of Bhuiyan et al.(2000) results. The breadth (b) of flat plate obstruction used in this experiment was 25 mm. The flat plate breadth (b) to test channel width (w) ratio (b/w) was 1.0. Bhuiyan et al.(2000) carried out experiment with flat plate of 42 mm breadth and in that case breadth to test channel width ratio (b/w) was seen to be 1.68. Bhuiyan et al.(2000) used a different open channel rig to carry out the experiment where height of the water was varied with flow rate. Present study is involved with a detailed investigation of more parameters and was undertaken in a new open channel rig where depth of fluid was maintained constant at different velocities.

5. Conclusion

From this investigation it is observed that the flow in the channel placed in another wider channel with obstruction geometry at the entry can be stagnant, reverse or forward. Flow behavior inside the test channel depends on the position of the obstruction geometry (g), the length of the test channel (L) and the Reynolds number (Re). The maximum reverse flow was observed at g/w ratio of 1.5 for range of Reynolds numbers of 1000 to 9000. The reverse flow inside the test channel was observed around 20% to 60% of the outside test channel velocity. The maximum forward flow inside the test channel was observed 65% to 80% for Reynolds number ranging from 1000 to 9000.

For lower and higher g/w ratio (except for g/w=2) the flow trend is almost unaffected by L/w ratios. The dramatic change of reverse flow to forward flow was reported at L/w ratio of 14 and for g/w ratio 2. The reverse flow was observed at Reynolds number ranges from 1000 to 9000 for low g/w ratio whereas forward flow was observed for higher g/w ratio.

It can be concluded that the flow in the test channel is strongly governed by the location of the obstruction geometry and the Reynolds number. The combination of the negative pressure behind the flat plate and the vortex shedding at the entrance determined the magnitude of the reverse flow. It should be noted that the emphasis of this study is on the flow pattern and phenomenon of flow inside and around the test channel and further study is recommended for detailed investigation into the dynamics of vortex and turbulence of the flow.

Acknowledgment

Authors gratefully acknowledge the financial support provided by the James Goldston Faculty of Engineering and Physical Systems, CQU, Australia for this study. Authors would like to thank Mr. Ray Kearney and Mr. Gary Hoare for the fabrication of the open channel rig, and Mr.

Duncane Bourne and Dr. Col Greensil for their assistance in flow visualization photography.

References

Abernathy, F. H. and Kronauer, R. E., 1962, "The Formation of Vortex Streets," *J. of Fluid Mech.*, Vol. 13, pp. 1~20.

Bearman, P. W. and Trueman, D. M., 1972, "An Investigation of the Flow Around Rectangular Cylinders," *Aeronautical Quart*, Vol. 23, pp. 229~237.

Bhuiyan, M. A. Khan, M. M. K. and Kabir, M. A., 2000, "Reverse Flow of a Non-Newtonian Fluid in a Channel," *Rheology Congress*, Cambridge, U. K Vol. -3, pp. 417~418.

Davis, C. G. and Sorenson, K. E., 1969, "Handbook of Applied Hydraulics," *McGraw-Hill Co*, Canada

Eom, K., 1988, "Performance of Butterfly Valves as a Flow Controller," *J. of Fluids Eng.*, Vol. 100, pp. 16~19.

Gerrard, J. H., 1966, "The Mechanics of the Formation Region of Vortices Behind Bluff Bodies," *J. of Fluid. Mech.*, Vol. 25, pp. 401~413.

Gerrard, J. H., 1978, "The Wakes of Cylindrical Bluff Bodies at Low Reynolds Numbers," *Phil. Trans. R. Soc.*, London, A 288, pp. 351~382.

Gowda, B. H. L., Tulapurkara, E. G. and Swain, S. K., 1993, "Reverse Flow in Channel-Influence of Obstruction Geometry," *Experiments in Fluids*, Vol. 16, pp. 137~145.

Gowda, B. H. L. and Tulapurkara, E. G., 1989, "Reverse Flow in Channel with an Obstruction at the Entry," *Journal of Fluid Mech.*, Vol. 204, pp. 229~244.

Kabir, M. A., Khan, M. M. K. and Rasul, M. A., 2002, "Flow of Water in a Channel with Various Obstruction Geometries at the Entry," *2nd World Engineering Congress*, Sarawak, Malaysia.

Park, J. S., Kim, M. S., Lee, J. S and Lee, W. I., 2002, "A Semi-Implicit Method for the Analysis of Two-Dimensional Fluid Flow with Moving Free Surfaces," *KSME International Journal*, Vol. 16, No. 5, pp. 720~731.

Streeter, V. L., 1961, "Handbook of Fluid Dynamics," *McGraw-Hill Co*, Canada.

Val Healy, J., 1992, "Control of Turbulent Flow on a Backward Facing Step," *AIAA Paper*, 92-0066.

Unal, M. F. and Rockwell, D., 1988a, "On Vortex Formation from Cylinder Part 1. The Initial Instability," *J. of Fluid Mech.*, Vol. 190, pp. 491~512.

Unal, M. F. and Rockwell, D., 1988b, "On Vortex Formation from Cylinder. Part 2. Control by Splitter-Plate Interference," *J. of Fluid Mech.*, Vol. 190, pp. 513~292.

You, J. Choi, H. and Yoo, J. Y., 2000, "A Modified Fractional Step Method of Keeping a Constant Mass Flow Rate in Fully Developed Channel and Pipe Flows," *KSME International Journal*, Vol. 14, No. 5, pp. 547~552.